Alkali Metal Cation–Induced Destabilization of Gas-Phase Protein–Ligand Complexes: Consequences and Prevention

ARTICLE *in* ANALYTICAL CHEMISTRY · AUGUST 2011

Impact Factor: 5.64 · DOI: 10.1021/ac201686f · Source: PubMed

2 AUTHORS, INCLUDING:

Jonathan T S Hopper
University of Oxford
13 PUBLICATIONS **210** CITATIONS

analytical chemistry

ARTICLE

pubs.acs.org/ac

Alkali Metal Cation-Induced Destabilization of Gas-Phase Protein−Ligand Complexes: Consequences and Prevention

Jonathan T. S. Hopper and Neil J. Oldham*

School of Chemistry, University of Nottingham, University Park, Nottingham, NG7 2RD

Supporting Information

ABSTRACT: Electrospray ionization, now a well established technique for studying noncovalent protein−ligand interactions, is prone to production of alkali metal adducts. Here it is shown that this adduction significantly destabilizes the interactions between two model proteins and their ligands and that destabilization correlates with cation size. For both the [FKBP·FK506] and [lysozyme·NAG$_n$] systems, dissociation of the metalated complex occurs at markedly lower collision energies than their purely protonated equivalents. Dependency upon size of the metal$^+$ demonstrates the importance of electrostatic charge density during the dissociation process. Differences in the gas phase basicities (GBapp) of the multiply charged protein ions and proton and sodium affinities of the ligands explain the observed charge partitioning during dissociation of the complexes. Ion mobility-mass spectrometry measurements demonstrate that metal cation adduction does not induce a significant increase in unfolding of the polypeptides, indicating that this is not the principal mechanism responsible for destabilization. Destabilizing effects can be largely reduced by exposing the electrospray to solvent (e.g., acetonitrile) vapor, a method that acts to reduce the amount of adduct formation as well as decrease the charge states of the resulting ions. This approach leads to more accurate determination of apparent K_Ds in the presence of trace alkali metals.

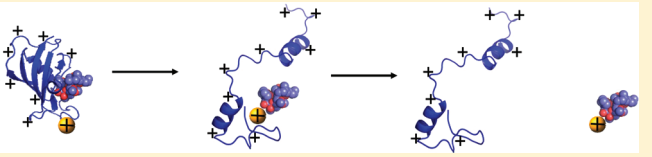

Electrospray ionization (ESI) of proteins from aqueous solutions containing volatile buffers allows the preservation of noncovalent interactions in the gas-phase.[1−3] Protein−protein and protein−ligand (P·L) complexes are capable of surviving desolvation and transmission into a high vacuum, permitting their direct detection by mass spectrometry (MS).[4] In its application to the study of biological noncovalent interactions, ESI-MS has several advantages over other biophysical techniques, including sensitivity and speed. Additionally, MS allows direct identification of individual binding components and their stoichiometry through measurement of discrete m/z values. Numerous studies have determined binding affinities from ESI-MS measurement through titration and competition assays.[5−9] Central to the success of the ESI-MS method in general, and its use in affinity measurement in particular, is the minimization of gas-phase ion dissociation. Postdesolvation loss of ligands from the P·L complex is irreversible and results in underestimation of the association constant K_A or, in extreme cases, failure to observe any binding. This is particularly problematic where interactions rely upon complementary enthalpic London dispersion forces and entropic hydrophobic effects, as the latter are largely absent in the gas phase. The reduced stability of nonpolar interactions in the gas phase is well-established[10] and contrasts with the generally high stability of ionic interactions.[11,12] Such effects may open the way to discrepancies between solution and gas phase measurements, although recent work has demonstrated that, with amphiphilic ligands, both hydrophilic and hydrophobic regions contribute to the stability of the P·L complex, indicating that the interactions of hydrophobic moieties are not invisible to mass spectrometry.[13,14]

Several strategies may be employed to minimize gas-phase P·L dissociation: including the use of collisional cooling and minimal acceleration potentials, both of which have the effect of lowering ion kinetic energy.[15−17] Alternatively, kinetic energy of the ions can be decreased by reducing the net charge acquired by the analytes during the electrospray process. This is believed to have the added benefit of producing more "native-like" ions.[18] Various methodologies have been developed in order to decrease the charge states of ions formed by electrospray. These include ion−molecule reactions,[19,20] ion−ion reactions,[21−23] and solution based additives.[24−26]

A recent example of a solution based additive is imidazole. The use of imidazole has allowed the detection of weak interactions, such as those seen between trypsin and its inhibitor benzamidine.[27] Imidazole may be added to the protein−ligand solution or introduced into the ESI source as a neutral spray.[28] In addition to reducing charge state, the additive is believed to provide a significant evaporative cooling effect on the ions of interest. A very recent paper by Ruotolo and co-workers demonstrates that buffer anions may be used to protect protein complexes in the gas-phase through a similar mechanism.[29] The use of electrosonicspray ionization (ESSI) also serves to stabilize noncovalent complexes through additional evaporative cooling.[30−32] In a comparison of ESI, nanospray, and ESSI methods for the determination of P·L K_Ds, it was found that ESSI gave results closest to the literature values

Received: June 30, 2011
Accepted: August 24, 2011
Published: August 24, 2011

in solution, suggesting that the ESSI supersonic nebulizer gas results in cooler gas-phase ions and less dissociation.[33]

The principal factor contributing to active destabilization of P·L complexes is Coulomb repulsion between like charges on the protein and ligand. The effect is clearly illustrated by the gas phase dissociation of ferri- and ferro-myoglobin ions, where the heme iron exists as Fe^{3+} and Fe^{2+}, respectively.[34] In the case of ferri-myoglobin, the heme ligand leaves with a net positive charge, whereas the reduced form of the protein dissociates through loss of an overall neutral ligand, with deprotonation of the two heme carboxylate groups balancing the Fe^{2+} charge. The energetics of P·L dissociation vary markedly between the two oxidation states, with the average increase in internal energy (ΔE_{INT}) of 183 and 290 eV required for 50% dissociation of the cationic ferri- and ferro-myoglobin complexes, respectively.[35] This difference is attributed to Coulomb release upon loss of positively charged ligand from the ferri-myoglobin, lowering the activation barrier for dissociation.

Positive ion ESI is highly sensitive to the presence of alkali metal cations such as Na^+ and K^+. Metal adducts of sample ions $[M + nH + m\text{metal}]^{(n+m)+}$ are commonly observed, even at trace levels of salt, and at higher concentrations salt clusters can dominate the spectrum. Multiply charged protein ions sprayed from neutral buffers are particularly susceptible to the attachment of sodium and potassium ions, showing multiple adduction in the presence of trace amounts of salt. The presence of alkali metals in peptides has been shown to induce significant structural rearrangement.[36] Ion mobility analysis of sodiated bradykinin and kemptide exhibited average collision cross sections which were notably smaller than their protonated counterparts and concluded that the sodium cation interacts with functional groups on the peptide backbone which act to stabilize the gas-phase structure.[37] Similar effects have also been observed in tryptic peptides which contain a significant number of carbonyl groups effectively solvating the alkali cations forming tight globular structures.[38]

Here we show that P·L complexes exhibiting alkali metal adducts dissociate at markedly lower energy than their purely protonated counterparts and discuss models for P·L dissociation in the gas-phase, which explains these observations. We provide evidence that this effect is only present as a gas-phase phenomenon and demonstrate a simple method for reducing both adduction and charge state which increases the stability of P·L complex ions, providing a better approximation of solution affinities.

MATERIALS AND METHODS

Mass Spectrometry/Ion Mobility. Electrospray and electrosonic spray ionization-ion mobility-mass spectrometry was performed on a Waters (Altrincham, U.K.) Synapt high definition mass spectrometer (HDMS), a hybrid quadrupole/ion mobility/orthogonal acceleration time-of-flight (oa-TOF) instrument. Samples were infused to the standard electrospray (z-spray) source using a Harvard apparatus 22 dual syringe pump, model 55-2222 and a 100 μL Hamilton syringe connected to a standard Waters ESI probe or a homemade ESSI probe, at infusion rates between 3 and 5 μL/min. The capillary of the ESI source was typically held at voltages between 2.5 and 3 kV and the ESSI probe at 4 kV, with the source operating in the positive ion mode. The sample cone was operated at 10−20 V, required to avoid gas-phase unfolding and preserve noncovalent interactions. The trap T-wave collisional cell, located prior to the drift tube, contained argon gas held at a pressure of 2.5×10^{-2} mbar. The ion mobility separator, utilizing nitrogen gas at 0.45 mbar and ambient temperature, employed a series of dc voltage waves (7 V wave height traveling at 280 m/s) to achieve mobility separation. Calibration of the traveling wave ion mobility spectrometer was performed as described in the literature.[39] The oa-TOF-MS was operated over the scanning range of m/z 500−3500 at a pressure of 1.8×10^{-6} mbar.

Collisional activation was used to investigate the gas phase dissociation behavior of the protein−ligand complexes. Activation of the quadrupole isolated ions was carried out in the "trap" region (a T-Wave cell located immediately before the ion mobility cell) of the Synapt MS by collision with argon gas at 2.5×10^{-2} mbar. By adjustment of the "trap" collision energy voltage, controlling the potential offset between the source ion guide and the "trap" region, the kinetic energies of ions entering the "trap" could be controlled. Dissociation profiles were constructed from stepwise increments in collision energy applied to the "trap" and the resulting mass spectra. For protein−ligand systems investigated here, data were acquired initially at 5 V increments, starting at 5 V. At voltage regions resulting in approximately 50% dissociation, additional intermediate voltages were employed between the 5 V steps to ensure more precise determination of Ec_{50} values (collision energy required to reduce the precursor relative intensity to 50% of its initial value). Spectra obtained at each energy value were averaged over at least 60 scans (1 scan/min). Upper voltage limits were considered to be where dissociation was complete. Data were plotted as the relative dissociation of the precursor (% precursor) against E_{LAB} collision energy and fitted as sigmoid curves and Ec_{50} values obtained from these plots. Sigmoid curves were fitted using origin software (OriginPro 8.1). The reproducibility of Ec_{50} values was determined by plotting five repeats of the $[FKBP \cdot FK506 + 7H]^{7+}$ complex. The mean of the obtained values were calculated and quoted along with its 95% confidence limits.

Precursor isolation of the lithiated complexes proved challenging. The m/z separation between the protonated and lithiated peaks for the protein−ligand systems being investigated was between 0.8 and 1.2, which could not be fully resolved using the quadrupole. To approximate the stability of the lithiated complexes, the quadrupole was set to the desired m/z value of the lithiated adduct. Increasing collision energy resulted in preferred dissociation of the lithiated complex over the protonated ions, evidenced by the appearance of the lithiated ligand signal. Therefore, it was possible to trace the dissociation of the lithiated complex before the onset of significant protonated dissociation. These initial values allowed construction and extrapolation of a sigmoid curve using the same fitting function as used with the other cation data sets.

Initially, in order to access a greater range of charge states than those available from the standard electrospray operating conditions, imidazole at a concentration of 10 mM was included in the sample. However, more control over charge state population was achieved by introducing solvent vapor into the source housing. A plastic cap containing solvent was placed into the source area and the door closed (see Figure S1 in the Supporting Information). When ESI is used, the position of the container within the source was found to influence the amount of charge reduction experienced, with the maximum effect observed with the vessel placed closer to the nebulizer jet. For these experiments, however, the container was placed just inside the doorway to the source chamber.

The K_a of a solution of known initial concentrations of protein ($[P]_0$) and ligand ($[L]_0$) was determined from the ratio (R) of the total intensity (I) of bound ($P{\cdot}L^{n+}$) and unbound (P^{n+}) using the protonated signals. These are given by eqs 1 and 2.[28]

$$K_A = \frac{R}{[L]_0 - \frac{R}{1+R}[P]_0} \quad (1)$$

$$R = \frac{\sum_n I(PL^{n+})}{\sum_n I(P^{n+})} \quad (2)$$

Sample Preparation. Lyophilized hen egg white lysozyme was obtained from Fluka (Gillingham, U.K.) and prepared as a 7 μM sample in 25 mM aqueous ammonium acetate. *N,N,N*-Triacetylchitotiose (NAG_3) and *N,N,N,N,N*-pentaacetylchitopentaose (NAG_5) were obtained from Sigma (Poole, U.K.) and prepared at 20 μM in the same solvent. To minimize the turnover of NAG_5, a dual syringe injection system was used by infusing the protein and the ligand through separate tubing and mixing via a PEEK "T-piece" just prior to the electrospray probe.

Recombinant human FK-binding protein (FK-BP) was expressed in *E. coli* (strain BL-21) from a plasmid kindly supplied by Dr. Sophie Jackson, University of Cambridge, U.K., following a similar protocol described elsewhere.[40] Aliquots (~1 mg mL^{-1} in thrombin cleavage buffer (see Supporting Information)) were desalted using Vivaspin (Epsom, U.K.) ultrafilters (molecular weight cutoff (MWCO) 3 000) and diluted to 5 μM in aqueous ammonium acetate (25 mM). FK-506 monohydrate was obtained from Sigma (Poole, U.K.) and was added to the FKBP sample at a 6 μM final concentration.

Alkali metal salts (LiOAc, NaOAc, KOAc, and CsOAc) were purchased from Sigma-Aldrich (Poole, U.K.) and added to the protein samples to a final concentration of 100 μM.

Fluorescence. Fluorescence measurements on lysozyme were conducted in 25 mM aqueous ammonium acetate with and without the addition of sodium acetate (100 mM). Excitation wavelength was set to 280 nm and was accompanied by an emission of the protein at a maximum of 348 nm. Addition of the NAG_3 ligand, chosen due to the low turnover rate of this substrate, resulted in a shift in emission to shorter wavelengths (337 nm) and increased emission intensity. Protein concentration in the pure ammonium acetate solution was 47.3 and 48.1 μM in the protein sample spiked with 100 mM sodium acetate. NAG_3 (5−150 μM) was titrated into each protein sample. Measurements were repeated five times, and the average intensity at each emission wavelength was calculated. Each scan was made between emission wavelengths of 300 and 500 nm with a scan speed of 200 nm min^{-1}. The excitation and emission slit widths were both set to 6 nm. To investigate whether enzymatic turnover occurred over the time period of the measurement, an equimolar amount of protein and NAG_3 were added to the cuvette and the emission spectrum was recorded every minute for 45 min. No turnover of substrate was detected on this time frame, confirming that the titration experiment could be carried out by making subsequent additions of the NAG_3 and treating it as a stable ligand.

An emission wavelength of 322.5 nm exhibited the greatest separation between the lysozyme and lysozyme·NAG_3 emission intensities. The difference between the intensity obtained at each NAG_3 concentration and the original unbound protein signal at this wavelength was normalized (B). Data obtained for the lysozyme·NAG_3 system were fitted using the linearized Langmuir plot which allows the K_D of a particular system to be obtained by plotting the reciprocal of the ligand concentration against the reciprocal of the normalized intensity difference, B, according to eq 3.[41]

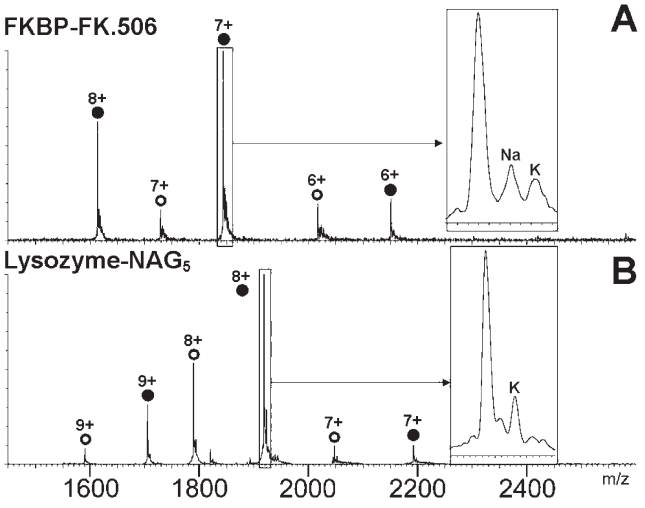

Figure 1. ESI-MS spectra of the (A) FKBP·FK506 and (B) lysozyme·NAG_5 complexes sprayed from 25 mM ammonium acetate. Solid circles represent bound protein−ligand complex and hollow circles indicate unbound protein (no unbound 8+ FKBP was observed). A zoomed window has been included for the most intense signal in each spectrum to illustrate the presence of adducts, attributed to sodium and potassium in these examples.

$$\frac{1}{B} = \left(\frac{K_D}{n}\right)\frac{1}{[L]} + \frac{1}{n} \quad (3)$$

Molecular Modeling. Ground state equilibrium geometry bond lengths for the M−N bond in metalated guanidine (where M = H, Li, Na, K, Cs) were calculated using semi empirical methods with the Spartan molecular modeling package (Waveform Inc., Irvine). These values were used to approximate the internuclear distance r in the M−N bond of the arginine side chain. This amino acid was chosen as it has the highest proton and sodium affinity of the 20 protogenic amino acids (AAs).

RESULTS AND DISCUSSION

Dissociation of Protonated vs Monosodiated Protein−Ligand Complexes. An ESI-MS spectrum of the FKBP·FK506 protein−ligand complex obtained from 25 mM ammonium acetate solution exhibited a narrow charge state distribution, consisting of the 6+, 7+, and 8+ ions, indicative of a compact structure. This was confirmed using T-wave ion mobility measurements, with measured cross sections in good agreement to that calculated from the solution structure using the trajectory model.[42] Common to many ESI spectra, the protonated signals were also accompanied by metal ion adducts. These arise from cations such as Na^+ and K^+, often present at trace levels within the sample solution and gained by the analyte during the ESI process (see Figure 1A).

Quadrupole separation of the $[FKBP{\cdot}FK506 + 7H]^{7+}$ complex and its monosodiated analogue $[FKBP{\cdot}FK506 + 6H + Na]^{7+}$ followed by collisional activation in the "trap" region of the

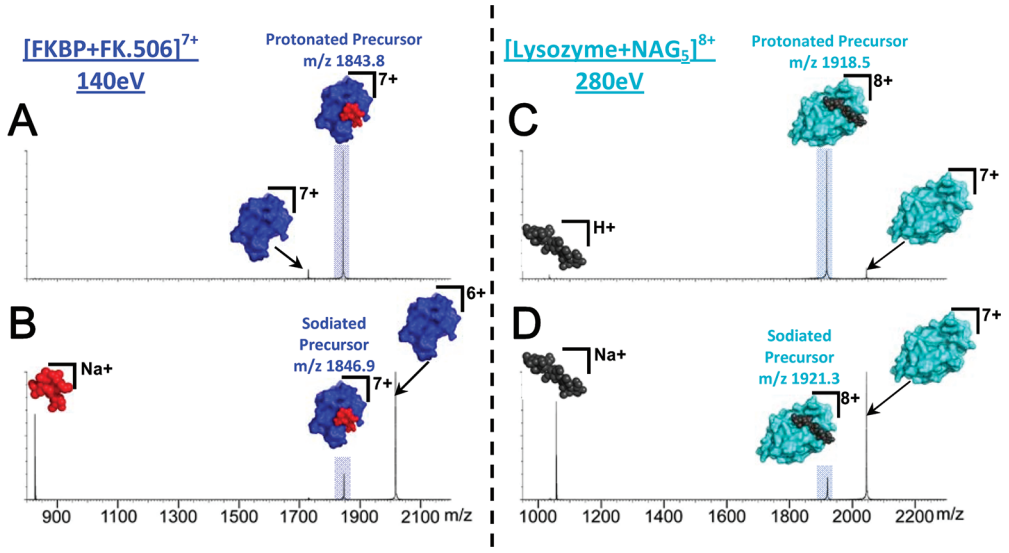

Figure 2. ESI-MS/MS spectra of protonated and sodiated FKBP·FK506 7+ complex (spectra A and B, respectively) at a collision energy of 140 eV and of protonated and sodiated lysozyme·NAG_5 8+ complex (spectra C and D, respectively) at a collision energy of 280 eV. Both systems show that the gas-phase stability of the monosodiated adduct is severely disrupted with respect to the protonated complex.

instrument led to disruption of the P·L complexes. Figure 2A illustrates that raising the E_{lab} collision energy to 140 eV resulted in the onset (7%) of dissociation in the $[FKBP·FK506 + 7H]^{7+}$ complex by a mechanism that proceeds via the loss of neutral FK506. Subjecting the $[FKBP·FK506 + 6H + Na]^{7+}$ complex to the same collision energy, however, resulted in almost complete dissociation of the precursor (83% dissociation) and loss of charged/sodiated FK506, resulting in an apoprotein product ion possessing reduced charge ($[FKBP + 6H]^{6+}$, see Figure 2B).

The loss of a charged, sodiated ligand from the $[FKBP·FK506 + 6H + Na]^{7+}$ complex versus a neutral ligand from the $[FKBP·FK506 + 7H]^{7+}$ ion indicated a marked difference in the proton and sodium affinities of FK506 ligand relative to the protein. The increased affinity of the FK506 toward sodium (relative to a proton) would appear to account for destabilization of the sodiated complex through Coulombic effects, analogous to those seen with ferri-and ferro-myoglobin.[35]

The effect was further examined by investigating the dissociation behavior of protonated vs sodiated lysozyme·NAG_5 complexes. This system was chosen as, unlike FKBP·FK506, loss of charged ligand occurs from the purely protonated as well as the monosodiated P·L complex. With the use of the kinetic method,[43] the gas-phase basicity (GB) of NAG_5 was measured to be approximately 222 kcal mol^{-1}. The 8+ charge state of lysozyme has a gas-phase basicity of only 202.5 kcal mol^{-1},[20] explaining why charged ligand loss is observed for the protonated complex.

Assuming a simple charge-repulsion model is sufficient to explain the observed effect, then dissociation behavior of the protonated and monosodiated lysozyme complexes would be expected to be similar, since the net charge obtained by the ligand would be the same. ESI-MS of the lysozyme·NAG_5 complex, under the conditions described (see Materials and Methods), resulted in a narrow charge state distribution, consisting of the 8+ and 9+ charge states for both the bound and unbound forms of the protein (Figure 1B). The major charge state, namely, the 8+, was isolated and the protonated and monosodiated lysozyme·NAG_5 complexes were individually subjected to increased collisional activation. At an acceleration voltage of 35 V (280 eV translational kinetic energy for the 8+ species), 8% dissociation of the protonated complex was observed, producing a charged (protonated) ligand, as predicted by the GB values (see Figure 2C). Collisional activation of $[lysozyme·NAG_5 + 7H + Na]^{8+}$ with an identical energy resulted in a loss of charged (sodiated) ligand (see Figure 2D). However in this instance, the fraction dissociated was much greater, with only 15% of the precursor remaining. These data demonstrate that a simple charge-ligand loss versus neutral-ligand loss model is insufficient to describe alkali metal-induced destabilization of P·L complexes.

To obtain a more complete representation of the dissociation behavior of the FKBP and lysozyme complexes, spectra were obtained over a range of collision voltages and the percentage of precursor remaining plotted against collision energy. From the resulting sigmoid curves, the Ec_{50} value was determined. The Ec_{50} value describes the kinetic energy required to induce 50% dissociation of the complex and, if the first derivative of the sigmoid is considered, the point which leads to maximum dissociation rate of the complex as a function of energy. A value of 189.2 ± 0.3 eV was obtained, based on a sample size of 5 and a 95% confidence limit. The Ec_{50} values obtained for the FKBP and lysozyme systems are presented in Table 1.

To determine whether the destabilizing effect of sodium ions was purely a gas-phase phenomenon, the consequences of high salt concentrations on P·L binding were examined in aqueous solution. Fluorescence spectroscopy was used to measure the dissociation constant of the lysozyme·NAG_3 complex by a ligand titration method. In ammonium acetate solution (25 mM), a K_D value of 52.0 ± 3.6 μM was determined for the complex, which fell to 26.5 ± 1.1 μM in the presence of NaCl (100 mM) (see Figure S2 in the Supporting Information). These results show a higher solution binding affinity for lysozyme·NAG upon addition of Na^+ ions, possibly by strengthening the hydrophobic interactions between protein and ligand. This effect is the reverse of gas-phase behavior. Thus, metal cation-induced destabilization observed in the MS is absent in solution.

Other Group I Cations and the Effect of Charge Density. To investigate the effects of other alkali metals on the stability of

Table 1. Protonated and Sodiated Ec_{50} Values Obtained for the Major Charge States of Each Protein−Ligand System Studied

	Ec_{50}		
	[lysozyme·NAG_3 + 8H] $^{8+}$	eV [lysozyme·NAG_5 + 8H] $^{8+}$	[FKBP·FK506] $^{7+}$
protonated complex	311.8	403.6	189.2
sodiated complex	199.2	225.0	101.4

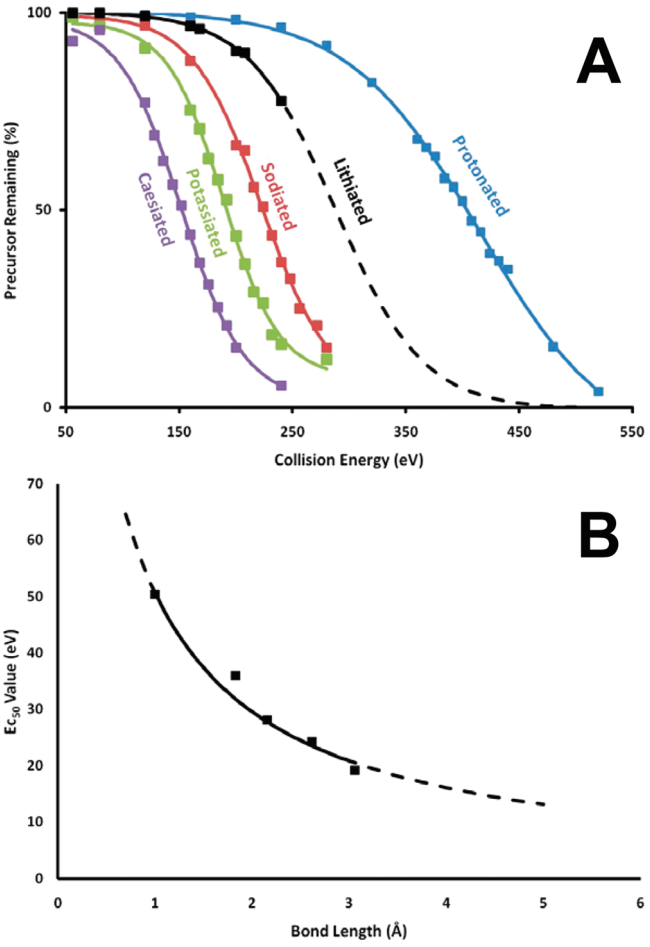

Figure 3. Dissociation data obtained for the lysozyme·NAG_5 (8+) complex. (A) Plot of collision energy against the degree of dissociation of [lysozyme·NAG_5 + metal]$^{8+}$, showing a sigmoidal depletion of the precursor ion intensity. (B) Ec_{50} values obtained from part A plotted against the internuclear distance for the metal−N bond in Arg, exhibiting an approximate $1/r$ correlation (dotted lines represent extrapolation of the line).

noncovalent protein−ligand complexes in the gas phase, samples of FKBP·FK506 and lysozyme·$NAG_{3\&5}$ were spiked with Li^+, Na^+ K^+, or Cs^+. Each of the monometalated adducts was then isolated and subjected to energy-programmed collisional activation. The survival of the precursor was monitored as described above, and the results are presented in Figure 3A.

Relative to the purely protonated species, the presence of all alkali metal-ion adducts reduced the gas-phase stability of the lysozyme·NAG_3, lysozyme·NAG_5, and FKBP·FK506 complexes studied. The amount of instability conferred increased with the size of the cation present, indicating a clear dependence on the electrostatic charge density during dissociation. To rationalize this effect, a simplified model was used to approximate the bond length between the metal and the protein amino acid side chains. Arg was chosen as the side chain, since this amino acid exhibits the highest sodium and proton affinities.[44] N-metal internuclear distances r were determined from a semiempirical equilibrium geometry calculation (see Molecular Modeling) of the metal-Arg side chain complex. When Ec_{50} values from Figure 3A were plotted against r for each metal, an approximate $1/r$ relationship was observed. This is in agreement with a Coulombically driven effect, where breaking metal−protein interactions controls the dissociative process. Clearly, modeling the metal−protein interactions based solely on Arg is a gross approximation, but the complexity of the total P·L system renders a more accurate description highly challenging. Moreover, the nature of the interactions formed between metal cation and Arg are believed to depend strongly on the cation's size. Recent work by Forbes et al. has demonstrated that smaller cations such as the proton and lithium prefer to exist in a "charge-solvated" environment, whereas the larger cations such as potassium and cesium interact with a zwitterion form of Arg.[45] Although these studies were conducted on the free amino acid, rather than its condensed form, it is likely that the amphiprotic properties of the proteins examined here would enable polydentate interactions and charge solvation vs zwitterion effects may be seen at the protein level.

The effect of alkali metal cation adduction was also investigated for a range of charge states of both protein systems. All charge states (6−9+ for lysozyme·NAG_3, lysozyme·NAG_5, and 6−8+ for FKBP·FK506) showed increased gas-phase destabilization as a function of alkali metal cation radius (Figures S3−S7 and Table S1 in the Supporting Information). For lysozyme·NAG_3, the 7+ charge state was most destabilized with all metals, whereas for lysozyme·NAG_5 the 8+ charge state was most affected. No significant destabilization as a function of charge was observed for the FKBP·FK506 complex.

An investigation of the complex between FKBP·FK506 and the divalent group II cations calcium and magnesium showed no detectable differences in dissociation energy relative to the purely protonated ion, suggesting destabilization is an effect of singly charged cations.

Previous studies concerning the effect of alkali metals on peptide ions provide evidence of significant conformational rearrangement.[36] Clearly, similar effects could occur in protein−ligand systems; however, ion mobility spectrometry (IMS) of the unactivated complexes did not reveal conformational differences even between the extreme protonated and caesiated protein cases (See Figure S8 in the Supporting Information). To investigate whether the presence of alkali metals lead to different unfolding pathways from those seen in the purely protonated complex, the ion mobility drift traces of protonated, sodiated, and potassiated precursors were compared for collision energies spanning the ligand dissociation event. For the protonated and metalated [lysozyme·NAG_5]$^{8+}$ precursor complex and dissociated protein products ([lysozyme]$^{7+}$), the ion mobility drift traces were identical (see Figures S9 and S10 in the Supporting Information). Similar results were also obtained for the [lysozyme·NAG_3]$^{8+}$ system (Figures S11 and S12 in the Supporting Information). For the [FKBP·FK506 + 6H + metal]$^{7+}$ complex, small differences were observed between precursor drift traces due to increased dissociation of the metalated

complexes at low collision energies, which in turn lead to more compact protein product ion conformations (see Figures S13 and S14 in the Supporting Information). Therefore, with respect to destabilization of the P·L complex, ion mobility measurements did not suggest a major role for metal-induced structural rearrangement.

The metal cation size-dependence seen during destabilization of P·L complexes indicates that adduction of a large cation lowers the activation barrier to dissociation. Possible mechanisms for this include (i) disruption of the protein−ligand native binding interface, (ii) disruption of the protein−ligand interaction in a dissociative transition state, and (iii) migration from protein to ligand prior to dissociation. The first mechanism would require trapping of the cation in the protein binding site or on the ligand surface before formation of the P·L interaction in solution. This seems unlikely, as the solution interaction of lysozyme and NAG_3 is actually enhanced by the presence of Na^+ ions. The second mechanism is more supported by the data, as structural rearrangement of the complex under collisional activation[42] would result in a protein·metal·ligand complex, where increasing the size of the bridging metal would reduce the stability of the ternary complex. Given the high metal ion affinity of the FK506 or NAG_n, the metal would generally leave with the ligand. The third explanation relies on cation transfer as the rate determining step; since as the metal-ion radius increases, the protein to ligand transfer would become more facile.[46] The resulting Coulombic repulsion between charged protein and charged ligand could then drive dissociation.[35] Indeed, a composite mechanism of (ii) and (iii) is also possible.

Significance and Prevention. The significance of alkali metal-induced destabilization lies in its potential to confound the detection of P·L complexes in the gas-phase. Weak interactions, for example, those driven primarily through hydrophobic contacts, may not be observed at all from samples with notable salt content or where the protein charge state is high. In cases where the complex is seen, the presence of the cations could prove a major source of error when using ESI-MS for obtaining apparent binding affinity data. The successful application of ESI-MS requires the preservation of P·L complexes in the gas-phase, a condition that may not be satisfied in the presence of alkali metals. Sodium and potassium ions are extremely common in aqueous samples. Cesium, although a rare background contaminant, may be observed if CsI clusters are used for mass calibration. Therefore, this study highlights the need for careful washing and effective desalting procedures of samples subjected to ESI-MS analysis.

Having identified this destabilization effect, caused by alkali metal-ion adduction in protein−ligand complexes, we next sought to reduce it. Two obvious approaches were considered: first, directly reducing the amount of alkali metal adduction and second, decreasing the internal energy of the P·L complex ions. The former may be achieved by thorough desalting and the latter by a reduction in kinetic energy acquired by the ions as they travel through the mass spectrometer, which in turn can be accomplished by decreasing the charge state of the ions. This has a secondary benefit of decreasing Coulombic repulsion within the P·L complex, known to be an important factor in destabilization. Decreasing the charge state may also act to reduce the effect by increasing the cation affinity of the protein and promoting a dissociation mechanism where the ligand is lost as a neutral. This would remove dissociative Coulomb release and act to stabilize the complex.

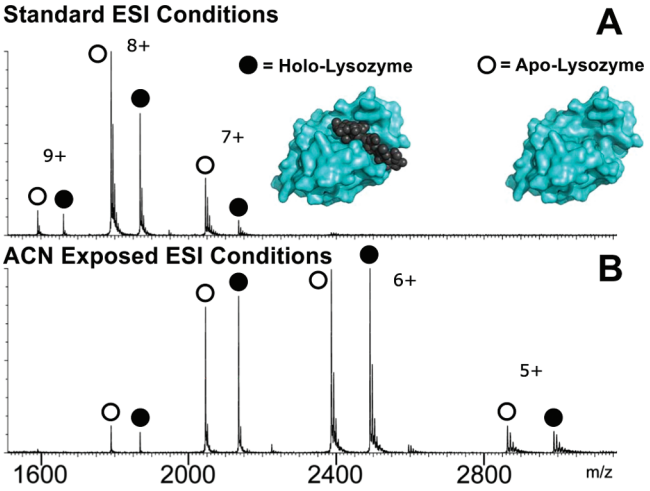

Figure 4. ESI-mass spectra acquired for lysozyme·NAG_3 (3.6 μM lysozyme and 10.8 μM NAG_3) under standard ESI conditions and in the presence of MeCN vapor (introduced in the source housing) in the presence of 100 μM KOAc. The addition of MeCN results in a lower charge state distribution and a decrease in the degree of adduction.

Several approaches presented in the literature describe innovative ways of either in-line desalting[47,48] of samples or methods to reduce the net charge accumulated by protein ions during ESI.[26] Studies in our laboratory have shown that exposure of ESI droplets to neutral vapor from solvents such as acetonitrile, methanol, and triethylamine are effective at reducing ESI charge states (see Figure 4). It should be noted that, unlike previously reported solvent vapor exposure methods, for example, Zenobi's[20] PA determination method, solvated/partially desolvated ions were utilized here. Electrosprayed droplets, not naked protein ions, were exposed to solvent vapor in the source housing. Our approach is closer to that utilized in a recent paper by Fenn et al.,[49] where electrospray droplets were exposed to solvent vapor introduced into the cone gas in order to study the ionization efficiency of singly charged peptides.

To demonstrate the benefit of solvent exposure in the reduction of alkali metal effects, the apparent dissociation constants of the lysozyme·NAG_3 complex were measured (see Materials and Methods for details). With the use of standard ESI conditions, a value of 16.4 ± 2.3 μM was obtained . This is somewhat higher than the literature value of 9.1 μM, measured in solution using fluorescence.[49] Figure 4A shows the standard ESI-mass spectrum obtained for lysozyme (3.6 μM) and NAG_3 (10.8 μM), used to measure the value above. The sample was deliberately spiked with 100 μM potassium acetate to produce significant adduction. At a ligand concentration close to the expected K_D, approximately 50% bound complex should be observed. This was not the case with the standard ESI spectrum, and unbound protein signals remained dominant. This is most likely due to gas-phase dissociation caused by the presence of potassium adducts. It was noticeable that lower charge states acquired more adducts during the electrospray process. While the highest charge state (9+) showed very little adduction, charge states 8+ and 7+ exhibited much more abundant adduct signals and depleted levels of bound complex. Such a result could explain the high apparent K_D value. While still infusing the same sample, a vial of acetonitrile was placed within the source housing (see Mass Spectrometry/Ion Mobility and Figure S1 in the Supporting Information).

The resulting spectrum is illustrated in Figure 4B, showing notably more bound lysozyme·NAG_3 complex was preserved. This may be due, in part, to a net reduction in the degree of potassium adduction when MeCN was present. In the absence of the solvent, 51% of the peaks were attributed to adducts; however, adding MeCN to the source reduced this to 38%. Additionally, the free ligand signal also showed a reduction in potassium adduction ($[NAG_3 + K]^+/[NAG_3 + H]^+ = 2.6$ in the absence of MeCN vapor and ~1 in the presence of MeCN). Adduct reduction has also been observed for numerous protein systems in our laboratory, and the example of FKBP is included in the Supporting Information (Figure S15). Perhaps the most significant benefit of solvent exposure was the reduction in charge state, which moved from an average of 7.9+ to 6.5+ following exposure to MeCN vapor. Since adducts were preferentially formed on lower charge states within a given distribution, the higher charges (8+ and 7+) were now almost completely free of metal ions. Lower charge states, which gained less internal energy within the instrument, were less susceptible to destabilization and little dissociation was observed for these species. A K_D of 9.2 ± 0.8 μM was determined under conditions of solvent exposure, which was significantly lower than that measured under standard conditions, and in very good agreement with the solution literature value.

Taken together, these results highlight that alkali metal adducts from the electrospray process can significantly destabilize protein−ligand complexes in the gas-phase. The effect is particularly problematic when measuring apparent K_Ds and may even prevent the observation of certain complexes by ESI-MS. We demonstrate that the size of the alkali metal cation correlates with the degree of destabilization induced and have proposed a charge migration mechanism which explains these observations. We have been able to demonstrate that these effects are exclusively present as a gas-phase phenomenon. Further, we present a solvent exposure method to minimize these effects through charge-state and adduct reduction. As ESI-MS methods find increasing application in the detection of protein noncovalent interactions, this study highlights a route to potential discrepancies between solution and gas-phase measurements. Providing care is taken to reduce alkali metal adduction and decrease protein charge state, it appears that these effects can be largely overcome.

■ ASSOCIATED CONTENT

Supporting Information. Additional information as noted in text. This material is available free of charge via the Internet at http://pubs.acs.org.

■ AUTHOR INFORMATION

Corresponding Author
*E-mail: neil.oldham@nottingham.ac.uk.

■ ACKNOWLEDGMENT

The authors would like to gratefully acknowledge Kleitos Sokratous for generous contributions and helpful discussions concerning charge state reduction and Jose Afonso, Joanne Stachen, and Dr. Robert Layfield for their time and assistance in the expression of FK-binding protein. Thanks to Elizabeth Morris and Professor Mark Searle for their assistance in acquiring fluorescence data. Also, thanks to Dr. Sophie Jackson who kindly supplied the plasmid for FK-binding protein. Finally thanks to the University of Nottingham and EPSRC for financial support.

■ REFERENCES

(1) Ganem, B.; Li, Y. T.; Henion, J. D. *J. Am. Chem. Soc.* **1991**, *113*, 7818–7819.
(2) Ganem, B.; Li, Y. T.; Henion, J. D. *J. Am. Chem. Soc.* **1991**, *113*, 6294–6296.
(3) Katta, V.; Chait, B. T. *J. Am. Chem. Soc.* **1991**, *113*, 8534–8535.
(4) Loo, J. A. *Mass Spectrom. Rev.* **1997**, *16*, 1–23.
(5) Daniel, J. M.; Friess, S. D.; Rajagopalan, S.; Wendt, S.; Zenobi, R. *Int. J. Mass Spectrom.* **2002**, *216*, 1–27.
(6) Wortmann, A.; Jecklin, M. C.; Touboul, D.; Badertscher, M.; Zenobi, R. *J. Mass Spectrom.* **2008**, *43*, 600–608.
(7) Mathur, S.; Badertscher, M.; Scott, M.; Zenobi, R. *Phys. Chem. Chem. Phys.* **2007**, *9*, 6187–6198.
(8) Bligh, S. W. A.; Haley, T.; Lowe, P. N. *J. Mol. Recognit.* **2003**, *16*, 139–147.
(9) Veros, C. T.; Oldham, N. J. *Rapid Commun. Mass Spectrom.* **2007**, *21*, 3505–3510.
(10) Robinson, C. V.; Chung, E. W.; Kragelund, B. B.; Knudsen, J.; Aplin, R. T.; Poulsen, F. M.; Dobson, C. M. *J. Am. Chem. Soc.* **1996**, *118*, 8646–8653.
(11) Xie, Y. M.; Zhang, J.; Yin, S.; Loo, J. A. *J. Am. Chem. Soc.* **2006**, *128*, 14432–14433.
(12) Yin, S.; Xie, Y. M.; Loo, J. A. *J. Am. Soc. Mass Spectrom.* **2008**, *19*, 1199–1208.
(13) Liu, L.; Bagal, D.; Kitova, E. N.; Schnier, P. D.; Klassen, J. S. *J. Am. Chem. Soc.* **2009**, *131*, 15980–15981.
(14) Barylyuk, K.; Balabin, R. M.; Grünstein, D.; Kikkeri, R.; Frankevich, V.; Seeberger, P. H.; Zenobi, R. *J. Am. Soc. Mass Spectrom.* **2011**, *22*, 1167–1177.
(15) Smith, J. C.; Siu, K. W. M.; Rafferty, S. P. *J. Am. Soc. Mass Spectrom.* **2004**, *15*, 629–638.
(16) Douglas, D. J. *J. Am. Soc. Mass Spectrom.* **1998**, *9*, 101–113.
(17) Sobott, F.; Hernandez, H.; McCammon, M. G.; Tito, M. A.; Robinson, C. V. *Anal. Chem.* **2002**, *74*, 1402–1407.
(18) Clemmer, D. E.; Hudgins, R. R.; Jarrold, M. F. *J. Am. Chem. Soc.* **1995**, *117*, 10141–10142.
(19) Winger, B. E.; Lightwahl, K. J.; Smith, R. D. *J. Am. Soc. Mass Spectrom.* **1992**, *3*, 624–630.
(20) Touboul, D.; Jecklin, M. C.; Zenobi, R. *J. Am. Soc. Mass Spectrom.* **2008**, *19*, 455–466.
(21) Loo, R. R. O.; Udseth, H. R.; Smith, R. D. *J. Phys. Chem.* **1991**, *95*, 6412–6415.
(22) Zhao, Q.; Soyk, M. W.; Schieffer, G. M.; Fuhrer, K.; Gonin, M. M.; Houk, R. S.; Badman, E. R. *J. Am. Soc. Mass Spectrom.* **2009**, *20*, 1549–1561.
(23) Zhao, Q.; Schieffer, G. M.; Soyk, M. W.; Anderson, T. J.; Houk, R. S.; Badman, E. R. *J. Am. Soc. Mass Spectrom.* **2010**, *21*, 1208–1217.
(24) Lemaire, D.; Marie, G.; Serani, L.; Laprevote, O. *Anal. Chem.* **2001**, *73*, 1699–1706.
(25) Halgand, F.; Laprevote, O. *Eur. J. Mass Spectrom.* **2001**, *7*, 433–439.
(26) Pagel, K.; Hyung, S. J.; Ruotolo, B. T.; Robinson, C. V. *Anal. Chem.* **2010**, *82*, 5363–5372.
(27) Sun, J.; Kitova, E.; Klassen, J. *Anal. Chem.* **2007**, *79*, 416–425.
(28) Bagal, D.; Kitova, E. N.; Liu, L.; El-Hawiet, A.; Schnier, P. D.; Klassen, J. S. *Anal. Chem.* **2009**, *81*, 7801–7806.
(29) Han, L.; Hyung, S. J.; Mayers, J. J. S.; Ruotolo, B. T. *J. Am. Chem. Soc.* **2011**, *133*, 11358–11367.
(30) Wiseman, J. M.; Takats, Z.; Gologan, B.; Davisson, V. J.; Cooks, R. G. *Angew. Chem., Int. Ed.* **2005**, *44*, 913–916.
(31) Takats, Z.; Wiseman, J. M.; Gologan, B.; Cooks, R. G. *Anal. Chem.* **2004**, *76*, 4050–4058.
(32) Sun, J. X.; Kitova, E. N.; Klassen, J. S. *Anal. Chem.* **2007**, *79*, 416–425.

(33) Jecklin, M. C.; Touboul, D.; Bovet, C.; Wortmann, A.; Zenobi, R. *J. Am. Soc. Mass Spectrom.* **2008**, *19*, 332–343.
(34) Chrisman, P. A.; Newton, K. A.; Reid, G. E.; Wells, J. M.; McLuckey, S. A. *Rapid Commun. Mass Spectrom.* **2001**, *15*, 2334–2340.
(35) Mark, K. J.; Douglas, D. J. *Rapid Commun. Mass Spectrom.* **2006**, *20*, 111–117.
(36) Solouki, T.; Fort, R. C.; Alomary, A.; Fattahi, A. *J. Am. Soc. Mass Spectrom.* **2001**, *12*, 1272–1285.
(37) Wu, C.; Klasmeier, J.; Hill, H. H. *Rapid Commun. Mass Spectrom.* **1999**, *13*, 1138–1142.
(38) Rozman, M.; Gaskell, S. J. *J. Mass Spectrom.* **2010**, *45*, 1409–1415.
(39) Duijin, E.; Barendregt, A.; Synowsky, S.; Versluis, C.; Heck, A. J. R. *J. Am. Chem. Soc.* **2009**, *4*, 1452–1459.
(40) Main, E. R. G.; Fulton, K. F.; Jackson, S. E. *J. Mol. Biol.* **1999**, *291*, 429–444.
(41) Copeland, R. A. *Enzymes: A Practical Introduction to Structure, Mechanism and Data Analysis*, 2nd ed.; Wiley-VCH, Inc.: New York, 2000.
(42) Hopper, J. T. S.; Oldham, N. J. *J. Am. Soc. Mass Spectrom.* **2009**, *20*, 1851–1858.
(43) Cooks, R. G.; Patrick, J. S.; Kotiaho, T.; McLuckey, S. A. *Mass Spectrom. Rev.* **1994**, *13*, 287–339.
(44) Kish, M. M.; Ohanessian, G.; Wesdemiotis, C. *Int. J. Mass Spectrom.* **2003**, *227*, 509–524.
(45) Forbes, M. W.; Bush, M. F.; Polfer, N. C.; Oomens, J.; Dunbar, R. C.; Williams, E. R.; Jockusch, R. A. *J. Phys. Chem. A* **2007**, *111*, 11759–11770.
(46) Tavasoli, E.; Fattahi, A. *J. Theor. Comput. Chem.* **2009**, *8*, 475–490.
(47) Boys, B. L.; Konermann, L. *J. Am. Soc. Mass Spectrom.* **2007**, *18*, 8–16.
(48) Chen, Y. J.; Mori, M.; Pastusek, A. C.; Schug, K. A.; Dasgupta, P. K. *Anal. Chem.* **2011**, *83*, 1015–1021.
(49) Nguyen, S.; Fenn, J. B. *Proc. Natl. Acad. Sci. U.S.A.* **2007**, *104*, 1111–1117.
(50) Schindler, M.; Assaf, Y.; Sharon, N.; Chipman, D. M. *Biochemistry* **1977**, *16*, 423–431.